Numerical strategies for the prediction of patterned wafer warpage during manufacturing process

Fabrice Roqueta, Mohamed Boutaleb, Phuc Viet Khoa Nguyen, Jean-Mathieu Mencik

Numerical strategies for the prediction of patterned wafer warpage during manufacturing process

Fabrice Roqueta[1], Mohamed Boutaleb[1], Phuc Viet Khoa Nguyen[2] and Jean-Mathieu Mencik[2]
[1] STMicroelectronics, APMS DFD, 10 Rue Thales de Milet, 37100 Tours, France
[2] INSA Centre Val de Loire, Laboratoire de Mécanique Gabriel Lamé, 41034 Blois, France
Corresponding author: fabrice.roqueta@st.com

Abstract

A manufacturing process consists of the deposit of thin films at different temperatures which produce in-plane stress loading. The presence of these mechanical stresses in different layers induces deformation of the wafer. In this sense, wafer warpage usually occurs which can cause unexpected large and critical deformations of the structure, including symmetrical (spherical) and asymmetrical deformed shapes. A wafer usually represents the repetition of many identical substructures (patterns) which are obtained by photo-lithography and etching steps. The magnitude of the deformed shape of a wafer could be high enough to prevent the manufacturing process. Then the prediction of the warpage phenomenon becomes crucial at the early stage of the design process. To predict wafer deformation accurately, analytical approaches do not seem suitable whereas standard finite element techniques based on 3D elements require excessive computational resources. Efficient alternative numerical approaches are therefore needed for the prediction of wafer warpage at affordable times. In this paper, comparisons are proposed between two kinds of alternative approaches, namely the homogenization technique and the FETI-DP method. Numerical simulations conducted on simple test-cases show that both these approaches are promising to achieve accurate results and strong time reduction compared to a full 3D analysis.

Keywords: *wafer warpage, patterned wafer, Finite Element Analysis, Homogenization, wafer scale*

1. Introduction

A microelectronics manufacturing process involves the use of large-scale wafers. As the semiconductor industry continues to evolve, the demand for even larger wafers becomes obvious in the future. The manufacturing process of microelectronics components requires the deposition of several thin films at different temperatures on a wafer substrate that generally consists of silicon. Because of the temperature changes involved in the manufacturing process, thermomechanical stresses occur due to mismatch between the thermomechanical material properties of the stack, e.g., the coefficient of thermal expansion (CTE). These thermomechanical stresses induce mechanical deformation commonly referred to as “wafer bow” or “wafer warpage”.

This phenomenon, widely known in the semiconductor industry, remains problematic especially for high levels of warpage. This can lead to several issues, particularly in line with the manufacturing process itself, such as wafer handling by automated systems or other key process steps such as photo-lithography. This highlights the need to predict wafer warpage and provide appropriate solutions to these situations.

In this context, several researchers have focused on studying the deformation of wafers during a manufacturing process. In the early 20th century, Stoney studied the deflection of a substrate (steel rule) on which a thin metal layer is deposited by electrolysis, and established a correlation between the stress levels and the induced curvature of the substrate [1]. This technique was adapted to the analysis of systems with circular shapes, such as wafers, and was extensively employed in the semiconductor manufacturing industry. Usual analytical and numerical approaches have proven accurate and reliable for modeling wafers uniformly coated with one thin film that exhibit low warpage and a linear behavior.

Several subsequent studies have aimed at widening the applicability of the Stoney model and addressing its limitations [2], [3], [4]. In [5], an analytical approach has been proposed that allows the deposition temperature of each film to be considered in an independent way, which yields the induced curvature of the system to be easily calculated.

Despite the recent advances in this field, the proposed approaches remain limited to systems with uniform deposits. In reality, film deposit undergoes diverse etching procedures leading to periodic patterns on the entire surface of a wafer. It is therefore crucial to take into account these patterns in the modeling and warpage calculation of wafers.

Although suitable and efficient to handle simple systems, analytical approaches suffers from strong limitations which make them irrelevant for predicting the deformation of patterned wafers especially for non-uniform pattern exhibiting complex geometric shapes. To address this issue, finite element (FE) approaches appear to be promising solutions. FE approaches include:

- 3D solid models, enabling a full geometric description of the structure. Although accurate, this approach

979-8-3503-9363-7/24/$31.00 ©2024 IEEE

however requires a huge number of degrees of freedom (DOFs) that lead to large-sized matrix systems and high CPU times.
- 2D axisymmetric models, which can be used for uniform coatings and depositions. However this approach is not suitable to describe periodic patterns.
- 2D shell models, which are good candidates to describe patterns with simple shapes. However, this approach fails to describe patterns with complex shapes.

For patterned films on substrates with complex patterns, both 3D models and shell models seem difficult to apply (as reported above). Alternative numerical approaches are therefore needed to predict complex patterned wafer warpage with accurate precision at low computational times. As periodic patterns are considered, homogenization approaches and domain decomposition approaches could be helpful by exploiting periodic conditions. Among the domain decomposition approaches is the FETI-DP (Finite Element Tearing and Interconnecting - Dual Primal) approach [6] which will be investigated in this paper.

In this paper, the performance of the homogenization technique and the FETI-DP approach for computing wafer warpage is investigated. Comparisons are carried out on simple structures where full 3D FE reference results are available.

2. Methodologies

As mentioned earlier, the focus here is on the analysis of substrates covered with patterned films (patterned wafers). As the patterns are periodically distributed on the substrates (see Figure 1), dedicated boundary conditions can be considered in order to restrict the analysis to that of a single cell, and subsequently propagate results (displacements and deformations) at the wafer scale. Within this framework, the homogenization technique and the FETI-DP approach can be used. For the sake of clarity, the methodologies involved in these two methods are described hereafter.

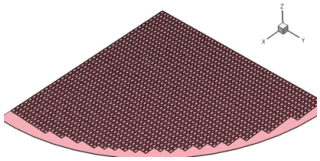

Figure 1. Example of a quarter wafer with patterned films.

A. Homogenization technique

Homogenization is a FE-based technique for modeling periodic structures. It is commonly employed in the fields of composite materials, laminated plates (stratified structures), and other systems that consist of the repetition of "unit cell" along one or more directions. Homogenization is particularly advantageous for modeling periodic structures, as it enables the determination of equivalent thermomechanical material properties for a representative volume element (RVE) of the whole structure. By approximating a periodic structure as a homogeneous material using effective material properties, the simulation of the entire structure can be conducted at a macroscopic scale.

The FE-based homogenization technique, as illustrated in Figure 2, involves subjecting a RVE to various perpendicular tensile, compressive and shear loadings. By computing the thermomechanical response of the RVE, the related equivalent thermomechanical material properties can be obtained through the constitutive Hooke's Law of orthotropic materials. Once these material properties are determined at the scale of the RVE, it becomes possible to approximate a whole pattern as an equivalent homogeneous layer with effective homogenized properties.

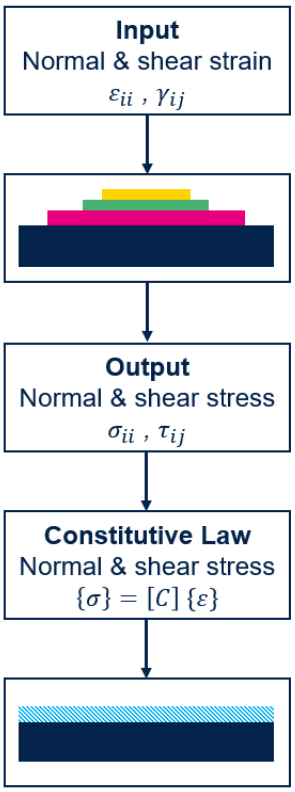

Figure 2. Principle of the homogenization technique.

B. FETI-DP Method

To address the lack of accuracy of the homogenization technique, domain decomposition methods can be considered, e.g., the FETI method in its dual-primal (DP) form [6]. The methodology of the FETI-DP method (see Figure 3) can be summarized as follows: (i) modeling of substructures (representative cells) via FE; (ii) assembling of the substructures at corners (primal assembly); (iii) solving small interface problems between the substructures via preconditioned conjugate gradient (PCG)

iterations. Since identical substructures are of concern, their stiffness matrix only needs to be computed once. Also, to reduce the size of the substructure FE models, a static/Guyan condensation of their stiffness matrix is considered. The FETI-DP method appears to be a good alternative to the classic FETI method where the corners are considered as interface DOFs (dual assembly), instead of being assembled in a preliminary step as in FETI-DP method (primal assembly). This prevents numerical issues associated with substructure rigid body modes.

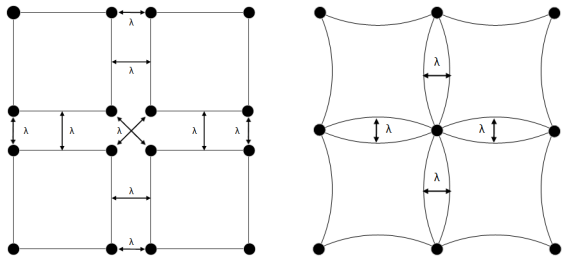

Figure 3. Substructures described with the FETI method (left) and the FETI-DP method (right).

3. Structure description

In order to compare the performances of the homogenization technique and the FETI-DP approach against the full FE method, two example structures are investigated. Here 2D periodic structures – i.e., structures composed of identical substructures along two $x-$ and $y-$directions – of square shape with symmetry conditions along two edges are considered. For comparison and computational purposes, structures with a small number of substructures (e.g. 3×3 substructures) with a moderately coarse mesh are considered. For the sake of clarity, the following terms are explained:

- Pattern: layout used to defined a substructure;
- Substructure: cell representing the substrate (with its entire thickness) and film(s) at the pattern scale (see Figure 4);
- RVE: equivalent cell representing the substrate (with a thickness which is percent of the total thickness) and film(s) at the pattern scale;
- structure: 2D periodic structure composed of identical substructures in the $x-$ and $y-$ directions (see Figure 4).

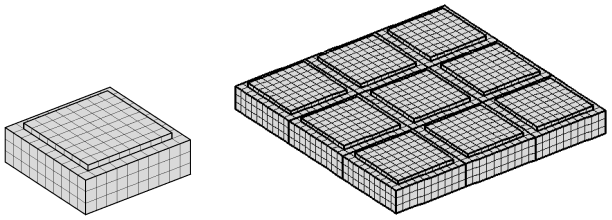

Figure 4. Schematics of a substructure (left) and a structure composed by 3×3 substructures (right).

In this paper, structures with 5×5, 10×10, 12×12, and 15×15 substructures are investigated. The related material properties are given in Table 1.

Material	Thickness (μm)	E (GPa)	ν	(ppm/°C)
Si	500	130	0.27	2.8
Film 1	1	69	0.33	24
Film 2	1	110	0.33	8.5

Table 1. Material properties of the substructures.

A. Substructure 1

In this case the substructures are composed of a substrate (1×1 cm^2) and one centered thin film of smaller dimensions (0.8×0.8 cm^2) as shown in Figure 5. The thicknesses of the substrate and the film are 500 μm and 1 μm, respectively. A substructure is meshed with eight-node brick elements including 40 elements on the edges of the substrate and 32 on the edges of the film. Also the substrate and the film are meshed using, respectively, two and one element layer along the thickness. This substructure mesh allows a good compromise between accuracy and efficiency. This FE mesh allows the computation of large structures (e.g., structures with 15×15 substructures to be performed at affordable times.

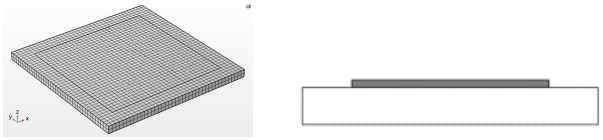

Figure 5. Schematic of substructure 1: 3D mesh (left) and cross section view (right).

B. Substructure 2

Substructures composed of a substrate with two centered thin films 1 and 2 of smaller dimensions are considered here (see Figure 6). The substrate has dimensions of 1×1 cm^2 and is 500 μm thick. The film 1 is located at the center of the substrate pattern with 0.6×0.6 cm^2 with a thickness of 1 μm. The film 2 has dimensions of 0.8×0.8 cm^2 (1 μm thick) is deposited on top of substrate and film 1 as shown in Figure 6. Again eight-node brick elements involving two element layers for the substrate and one element layer for the films are considered. In this case, the edges of the substrate, the film 1 and the film 2 are meshed with 40, 24 and 32 elements, respectively.

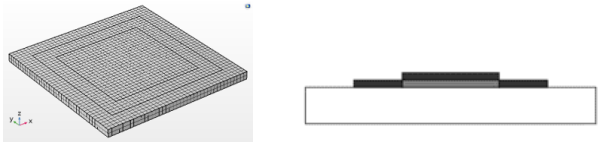

Figure 6. Schematic of substructure 2: 3D mesh (left) and cross section view (right).

4. Results and discussion

A. Modeling setup

The simulated structures represent a quarter of a whole periodic structure extending from 50 mm (5×5 substructures) to 150 mm (15×15 substructures). For each case, symmetry conditions are applied on two perpendicular edges (among the four structure edges) where the intersection point is supposed to be fixed as shown in Figure 7. The other two edges of the structure are supposed to be free. The mechanical loading results from a temperature step of 100°C applied on the whole structure. The static response of the structures are performed using a linear solver and 4 processors with 40 GB memory.

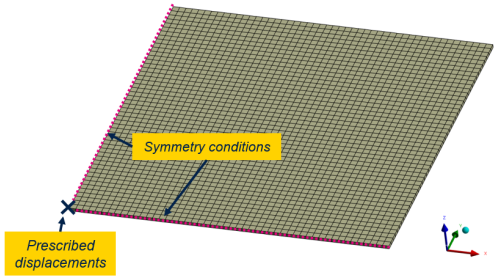

Figure 7. Boundary conditions of the structures.

B. 3D Solid vs. 2D Shell Approach

2D Shell approach consists on the modeling of a 3D structure with 2D shell elements with rotational displacement degrees of freedom. Those elements are based on Mindlin plate theory [7], [8]. This approach is relevant for structure with high aspect ratio. This approach allows to reduce significantly the number of DOF and then the calculation time. In these test-cases, structures are sufficiently simple to allow the use of 2D Shell due to low number of substructures included in the structures. As the shell elements are based on specific assumptions, simulations are done in order to quantify the discrepancy between those 2 approaches. Whatever the number of substructures, results for 2D Shell approach show an error of 11% compared to those obtained with a 3D solid element model. This decrease of accuracy is balanced by the calculation time. In fact, the calculation time for 2D Shell model is about seconds compared to calculation time for 3D solid model which is several hours strongly depending on the number of substructures in the structure.

As mentioned previously, the decrease of the DOF number in 2D Shell approach compared to 3D Solid approach leads to a strong decrease of calculation time (few seconds compared to several hours). However we can notice a loss of accuracy.

C. Homogenization technique

The transverse deflection of the structures under a temperature step of $\Delta T = 100$°C is assessed using the

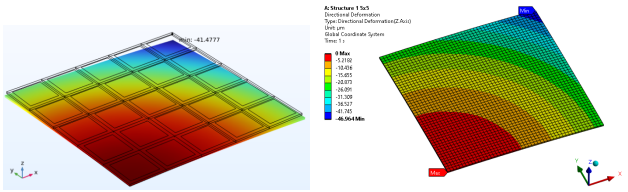

Figure 8. Z-displacement of the structure composed by 5×5 substructures: 3D solid model (left) and 2D shell model (right).

reference FE method and the homogenization technique. The homogenization technique has been described in Section 2. This first consists in determining a RVE of the periodic pattern of the wafer surface. This involves a substrate thickness ratio and the actual stack of the films (i.e., film 1 for structure 1, film 1 and film 2 for structure 2) as shown in Figure 9. This ratio is chosen so that it includes a thickness of 5% of the actual substrate thickness as illustrated in Figure 9 and Table 2. The in-plane dimensions of the RVE are similar to those of the substructures mentioned in Section 3. Once a RVE is determined, the homogenization process is performed to determine its equivalent thermomechanical properties through the application of various loading cases.

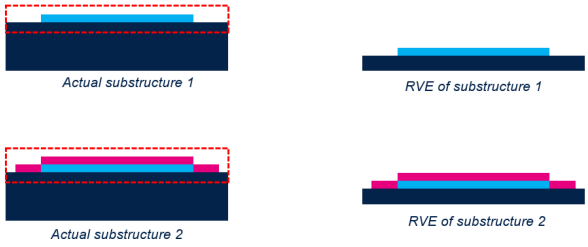

Figure 9. Representation (not to scale) of the substructure cross-section (right) and the equivalent RVE (left).

Substructure	**1**	**2**
Material	RVE thickness (μm)	
Substrate	25	25
Film 1	1	1
Film 2	NA	1

Table 2. Geometrical dimensions of the RVE (homogenization).

Taking the example of a normal tensile solicitation along x direction, a strain ε_{xx} is applied as displacements to the faces of the RVE normal to x. The reaction force values are then calculated which allows to obtain the corresponding stress values σ_{xx} along this direction. The elastic modulus E_x along x can thus be determined through the material constitutive laws $E_x = \frac{\sigma_{xx}}{\varepsilon_{xx}}$. Similarly, normal tensile tests along the $y-$ and $z-$directions are performed to calculate the elastic moduli E_y and E_z in

these directions. Poisson's ratios can thus be determined using the expression $\nu_{ij} = \frac{\varepsilon_{ii}}{\varepsilon_{jj}}$. Similarly, shear strains are applied using the same principle, thus allowing to determine shear moduli G_x, G_y and G_z of the RVE.

This homogenization procedure was applied to both substructures 1 and 2 in order to compute their orthotropic material properties. The finite element homogenization procedure was performed by leveraging the ANSYS Material Designer capabilities [9]. Table 3 summarizes the computed orthotropic homogenized material properties for substructures 1 and 2.

To simulate the entire structure, the patterns were substituted with a single equivalent layer having effective orthotropic material properties specified in Table 3. A 2D shell simulation was then conducted to determine deflection induced under thermal loading. This simulation took into account a substrate with a thickness equal to the actual thickness, but truncated by the substrate thickness used in the RVE modeling. Additionally, a layer with equivalent material properties was included in the simulation. The thickness of this layer matched that of the RVE. By exploiting the symmetries present in the models, only a quarter of the each geometry was simulated. As illustrated in Figure 7 the boundary conditions applied are such that the center of the geometry was fixed in terms of displacement, and the entire geometry undergoes a temperature change of $\Delta T = 100°C$. The results obtained for structures 1 and 2 are summarized in Table 4 and Table 5, respectively, and were compared to the results of the 3D Solid approach. Calculations of error and time reduction are based on the following equations:

$$err\% = \frac{{u_z}^{approach_i} - {u_z}^{3Dsolid}}{{u_z}^{3Dsolid}} \text{ and } \Delta t\% = \frac{|{t}^{approach_i} - {t}^{3Dsolid}|}{{t}^{3Dsolid}}.$$

Material properties	RVE Subtructure 1	RVE Substructure 2
E_{xx}, E_{yy} (GPa)	126.56	123.85
E_{zz} (GPa)	82.67	47.38
ν_{xy}	0.27	0.27
ν_{yz}, ν_{xz}	0.27	0.27
G_{xy} (GPa)	49.79	48.68
G_{yz}, G_{xz} (GPa)	0.35	0.04
α_{xx}, α_{yy} (ppm/°C)	3.10	3.09
α_{zz} (ppm/°C)	4.10	4.37

Table 3. Orthotropic homogenized material properties of RVE substructures 1 and 2.

The use of homogenization method coupled to 2D Shell approach allows to simulate structures with very quickly but without a significant factor due to the simplicity of our structures studied. A few loss of accuracy can also be noticed. For more complex structures, for example with a huge number of substructures, the homogenization method is relevant and allows the gain calculation time with a relative decrease of accuracy.

Approach	3D Solid		Homogenization		Comparison
Patterns	Disp. (μm)	Time (s)	Disp. (μm)	Time (s)	Error
5×5	-41.48	2706	-44.03	3	6.16%
10×10	-165.77	9140	-176.14	4	6.26%
12×12	-238.69	20119	-253.63	6	6.26%
15×15	-372.96	25432	-396.3	6	6.26%

Table 4. Comparison between 3D Solid and homogenization approach for structure 1

Approach	3D Solid		Homogenization		Comparison
Patterns	Disp. (μm)	Time (s)	Disp. (μm)	Time (s)	Error
5×5	-40.94	2764	-42.97	4	4.97%
10×10	-163.60	26721	-171.89	10	5.07%
12×12	-235.41	44253	-247.53	6	5.15%
15×15	-367.70	21195	-386.76	7	5.18%

Table 5. Comparison between 3D Solid and homogenization approach for structure 2

D. FETI-DP method

The FETI-DP method is used to compute the transverse displacements of structures 1 and 2 at one of the free corner. Comparisons with full 3D solid simulations are provided in Table 6 for structure 1 and Table 7 for structure 2. Results show that the FETI-DP solutions are in good agreement with those issued from full FE simulations. The FETI-DP method leads a very good balance between calculation time and accuracy. In fact, the accuracy loss is less than 1% compared to the 3D Solid simulations. The order of magnitude for the calculation times is several minutes compared to several hours in benefit of the FETI-DP method.

Approach	3D Solid		FETI-DP		Comparison
Patterns	Disp. (μm)	Time (s)	Disp. (μm)	Time (s)	Error
5×5	-41.48	2706	-41.55	180	0.17%
10×10	-165.77	9140	-166.10	157	0.20%
12×12	-238.69	20119	-239.10	170	0.17%
15×15	-372.96	25432	-373.60	195	0.17%

Table 6. Comparison between 3D Solid and FETI-DP approach for structure 1

Approach	3D Solid		FETI-DP		Comparison
Patterns	Disp. (μm)	Time (s)	Disp. (μm)	Time (s)	Error
5×5	-40.94	2764	-41.02	175	0.20%
10×10	-163.60	26721	-163.90	172	0.18%
12×12	-235.41	44253	-236.00	197	0.25%
15×15	-367.70	21195	-368.60	196	0.24%

Table 7. Comparison between 3D Solid and FETI-DP approach for structure 2

5. Conclusions

In this paper, the relevance of the homogenization technique and the FETI-DP method for modeling structures containing periodic patterns — which are relevant in semiconductor industry — has been discussed.

Within the framework of the homogenization technique, a RVE is used to calculate equivalent effective thermo-mechanical properties which are integrated into a 2D shell model. This leads the way to perform numerical simulations with low computational cost, with a relative loss of accuracy however.

Within the FETI framework, small interface problems for cells which rely on Lagrange multipliers can be quickly solved. This method has shown many advantages, e.g., for the modeling of silicon wafers in microelectronics. This yields small computational time as well as this prevents the issue of generating full FE structure meshes. It was observed that the FETI-DP method is much faster than the full 3D FE method while providing the same level of accuracy, as opposed to the homogenization technique where 2D shell element are invoked.

Follow-on works could concern model reduction strategies for the FETI-DP method, e.g., by expressing the Lagrange multiplier vectors at the substructure interfaces on low dimensional spaces. This open interesting prospects concerning the modeling and the efficient simulations of large-sized FE models. Other prospects could focus on nonlinear calculations, e.g., to handle geometrical or material nonlinear problems (plasticity) which are often encountered in industrial applications.

References

[1] G. G. Stoney, "The tension of metallic films deposited by electrolysis," *Proceedings of the Royal Society of London. Series A, Containing Papers of a Mathematical and Physical Character*, vol. 517, pp. 1858–1867, 1909.

[2] A. G. Evans and J. W. Hutchinson, "The thermomechanical integrity of thin films and multilayers," *Acta Metallurgica et Materialia*, vol. 43, pp. 2507–2530, 1995.

[3] C. H. Hsueh, "Thermal stresses in elastic multilayer systems," *Thin Solid Films*, vol. 418, pp. 182–188, 2002.

[4] S. Zhang, H. Zhang, and L. Zheng, "Residual stress of physical vapor-deposited polycrystalline multilayers," *Sci. China Phys. Mech. Astron.*, vol. 58, pp. 1–9, 2015.

[5] H. F. Miled, F. Roqueta, J. C. Craveur, E. L. Bourhis, P. Gardes, and A. Tougui, "Analytical multi-step homogenization methodology for a stack of thin films in microelectronics," in *2020 21st International Conference on Thermal, Mechanical and Multi-Physics Simulation and Experiments in Microelectronics and Microsystems (EuroSimE)*, pp. 1–7, 2020.

[6] C. Farhat, M. Lesoinne, P. LeTallec, K. Pierson, and D. Rixen, "Feti-dp: A dual-primal unified feti method-part i: A faster alternative to the two-level feti method," *International Journal for Numerical Methods in Engineering*, vol. 50, pp. 1523–1544, 2001.

[7] J. Schicker, T. Arnold, C. Hirschl, A. L. Iravani, and M. Kraft, "Simulation of the deformation behavior of large thin silicon wafers and comparison with experimental findings," in *2015 16th International Conference on Thermal, Mechanical and Multi-Physics Simulation and Experiments in Microelectronics and Microsystems (EuroSimE)*, pp. 1–6, 2015.

[8] J. Schicker, W. Khan, T. Arnold, and Hirschl, "Simulation the warping of thin coated si wafers using ansys layered shell elements," *Composite Structures*, vol. 140, pp. 668–674, 2016.

[9] ANSYS, "Material designer user's guide," 2024.